



University of HUDDERSFIELD

University of Huddersfield Repository

Kontogiorgos, Vassilis and Kasapis, Stefan

Modeling and fundamental aspects of structural relaxation in high-solid hydrocolloid systems

Original Citation

Kontogiorgos, Vassilis and Kasapis, Stefan (2016) Modeling and fundamental aspects of structural relaxation in high-solid hydrocolloid systems. *Food Hydrocolloids*. ISSN 0268-005X

This version is available at <http://eprints.hud.ac.uk/id/eprint/29824/>

The University Repository is a digital collection of the research output of the University, available on Open Access. Copyright and Moral Rights for the items on this site are retained by the individual author and/or other copyright owners. Users may access full items free of charge; copies of full text items generally can be reproduced, displayed or performed and given to third parties in any format or medium for personal research or study, educational or not-for-profit purposes without prior permission or charge, provided:

- The authors, title and full bibliographic details is credited in any copy;
- A hyperlink and/or URL is included for the original metadata page; and
- The content is not changed in any way.

For more information, including our policy and submission procedure, please contact the Repository Team at: E.mailbox@hud.ac.uk.

<http://eprints.hud.ac.uk/>

1
2
3
4
5
6
7
8
9
10
11
12
13
14
15
16
17
18
19
20
21
22
23

Modeling and fundamental aspects of structural relaxation in high-solid hydrocolloid systems

Vassilis Kontogiorgos¹ and Stefan Kasapis^{2*}

¹Department of Biological Sciences, The University of Huddersfield, Queensgate, HD1 3DH, UK

²School of Science, RMIT University, Bundoora West Campus, Plenty Road, Melbourne, Vic 3083, Australia

*Corresponding author

Email: stefan.kasapis@rmit.edu.au

Fax: +61 3 992 55241

Tel: +61 3 992 55244

24 **Abstract**

25 The structural relaxation properties of high-solid gelling polysaccharides, gelatin and
26 whey protein with small-molecule co-solutes have been reviewed focusing on the glass
27 transition region and glassy state of the mechanical master curve. Compliance with the
28 principle of thermorheological simplicity is established allowing horizontal superposition of
29 viscoelastic functions in the form of small-deformation stress relaxation or dynamic
30 oscillation modulus. Numerical calculations *via* the Tikhonov regularization yield smooth
31 stress relaxation spectra over a broad timescale that encompasses the isothermal process of
32 vitrification in these systems. Next, the molecular coupling theory addressed the polymer
33 chain dynamics of the local segmental motions that determine the glass transition temperature
34 (T_g) of condensed matrices. Thus a more complete picture of the physics of intermolecular
35 interactions in the short-time region of the glass dispersion has emerged. It allows estimation
36 of the relaxation time for local segmental motions at T_g , and the extent of cooperativity
37 between adjacent chemical moieties governing kinetics of viscoelastic relaxation in
38 hydrocolloid based systems at the glass transition region.

39

40

41 *Keywords: structural relaxation; Tikhonov regularization; relaxation time; glass transition;*
42 *molecular coupling theory.*

43

44

45

46

47 **1. Introduction**

48 Hydrocolloid chains have a large number of motions at different length scales due to the
49 plethora of monomers that result in numerous degrees of freedom. For instance, the rapid
50 local groups or segmental motions observed at the vicinity of the glass transition region of
51 concentrated preparations contrast vividly with the slow movements due to the reptation of
52 the entire chain along its contour in the elastomeric plateau response leading to the molecular
53 flow region of the viscoelastic master curve (Rubinstein & Semenov, 2001).

54 Molecular motion is of the utmost importance for the physical properties of
55 hydrocolloids, including viscoelasticity, diffusion and glass transition, which are controlled by
56 chain dynamics. Macromolecular motion, also termed structural relaxation, is accompanied by
57 changes in chain conformation leading to a reduction in chain stiffness, hence mechanical
58 network strength, and if allowed to proceed over a prolonged timescale of observation to
59 eventual molecular flow. It usually takes place over long times as different length-scale
60 components relax at characteristic times, τ . Timescales of various molecular motions can be
61 plotted on a relaxation spectrum that describe chain dynamics. As a result, relationships
62 between molecular structure and physical properties are drawn to optimize techno-
63 functionality.

64 Physicochemical techniques (e.g., NMR relaxation, light scattering, calorimetry etc.)
65 probe molecular motions at different length scales. Rheological tests, which are the interest in
66 this treatise, focus on motions occurring between 0.00628 – 628 rad/s although this range can
67 be extended with appropriate (horizontal only) superposition of data obtained at different
68 temperatures. In the following sections, we shall discuss approaches to calculate the relaxation
69 spectrum from rheological data underlined by prevalent schools of thought.

70 2. Calculation methods of relaxation spectra

71 Relaxation spectra cannot be measured directly but instead calculated from rheological
72 data, most commonly dynamic, creep or stress relaxation, performed in the linear viscoelastic
73 response of the material. Mechanical perturbations (e.g., stress) displace chains from their
74 equilibrium positions but they attempt to return to a thermodynamic stable state *via* an array
75 of molecular motions known as relaxations. The objective of calculating relaxation spectra is
76 to identify characteristic relaxation times (τ) with which polymeric chain-populations of
77 known molecular weight and fine structure relax to equilibrium. Correct identification of the
78 characteristic times is important, as it gives information on mechanical features at desired
79 temperatures of operation or storage that links to molecular architecture.

80 The process of extracting relaxation spectra is, mathematically speaking, an inverse
81 problem defined as the process of first obtaining the rheological responses (e.g., relaxation
82 modulus) and afterwards linking them to molecular motion. Fredholm integrals of the first-
83 kind are used to generalize the response of various viscoelastic functions:

$$84 \quad g(x) = \int_0^a K(x, \tau)H(\tau)d\tau, 0 \leq x \leq a \quad (1)$$

85 where, $g(x)$ is the measured signal and x is either t or ω for $G(t)$, $G'(\omega)$, $G''(\omega)$, and $H(\tau)$ is
86 the unknown solution that represents the continuous relaxation spectrum of the material.

87 Depending on rheological measurement, the kernel $K(x, \tau)$ is either $e^{-t/\tau}$, $(\omega^2\tau^2)/(1+\omega^2\tau^2)$
88 or $\omega\tau/(1+\omega^2\tau^2)$ for $G(t)$, $G'(\omega)$, $G''(\omega)$, respectively. Numerical calculation of $H(\tau)$ from
89 equation (1) results in ill-conditioned algebraic systems of equations, which means that small
90 perturbations in the measured signal $g(x)$ results in large deviations in the solution $H(\tau)$ (i.e.,
91 relaxation spectrum). If the ill-posed nature of the problem is overcome then the relaxation
92 spectrum can be calculated with accuracy and provide structural information for the material

93 under investigation. Early attempts to calculate the relaxation spectrum have been met with
94 numerical difficulties and the non-uniqueness of the solution (Ferry, 1980). To resolve such
95 problems, various algorithms that perform numerical calculations have been proposed over
96 the years. The major issue at hand is whether the resulting spectrum is a characteristic feature
97 of the material or an artifact of the algorithm. The desired properties of the algorithms have
98 been outlined in the literature (Winter, 1997) but an important characteristic of the calculation
99 process is the ability of several algorithms to return similar relaxation spectra (McDougall,
100 Orbey, & Dealy, 2014).

101 Various mathematical approaches have been proposed to calculate the relaxation spectra
102 of polymeric materials over the years (Baumgaertel & Winter, 1989; Elster & Honerkamp,
103 1991; Jensen, 2002; Provencher, 1982; Stadler & Bailly, 2009), and more recently (Bae &
104 Cho, 2015; Ciocci Brazzano, Pellizza, Matteo, & Sorichetti, 2016; Soo Cho & Woo Park,
105 2013). In practice, very few are used, as most are either proprietary information to the
106 researchers who developed them or a suitable computer program is not available. To
107 overcome these hurdles, regularization methods, attempting to calculate a smooth solution, are
108 commonly employed in the calculation of relaxation spectra. They incorporate ancillary
109 information about the attributes of the sought solution (e.g., non-negativity) and facilitate the
110 calculation of a meaningful spectrum (Elster, Honerkamp, & Weese, 1991).

111 In order to determine a relevant approximation of $H(\tau)$, the initial system of linear
112 equations describing the relaxation process is replaced with a set of equations that is less
113 sensitive to noise. Solution of the latter system of equations results in the best possible
114 approximation of $H(\tau)$, with the entire process being referred to as regularization. An
115 established methodology to numerically calculate the relaxation spectrum is through the

116 Tikhonov regularization (Tikhonov, Goncharsky, Stepanov, & Yagola, 1995). In common
117 least squares problems (e.g., linear regression for construction of a calibration curve), the
118 approach is to minimize the sum of squares of errors and arrive at the best approximate
119 solution (i.e., linear curve fitting). In ill-posed problems, the Tikhonov regularization favours
120 and achieves a desirable solution by including a regularization term in the minimization
121 process.

122 Utility of the regularization term is controlled by the regularization parameter, λ , which
123 plays a central role in successful calculations to yield the final relaxation spectrum. In
124 regularized calculations, the solution is dominated by two types of errors: the regularization
125 error caused by the numerical calculation and the perturbation error being inherent to
126 measurement (e.g, $G'(\omega)$ or $G(t)$). Choice of λ away from the optimum being either smaller,
127 with the perturbation error dominating the solution, or greater, with the regularization error
128 dominating the solution, result in either noisy spectra with a meaningless number of peaks or
129 over-smoothed solutions that lack information. For a fixed set of data, there is an optimal λ
130 that balances the two types of errors yielding the best $H(\tau)$ approximation. A common method
131 to find the optimum λ is with the aid of the L-curve criterion that addresses in the calculation
132 the two types of errors (Hansen, 1992; Rezghi & Hosseini, 2009).

133 Once the spectrum has been calculated, it is important to assess the range of relaxation
134 times that result in meaningful properties for the hydrocolloid system under investigation. It is
135 common practice to determine the relaxation spectrum within a reciprocal frequency range of
136 $\omega_{\max}^{-1} < \omega^{-1} < \omega_{\min}^{-1}$ for measurements that have been carried out at the corresponding
137 frequency range of $\omega_{\min} < \omega < \omega_{\max}$. However, this practice is incorrect due to various
138 experimental limitations associated with the rheological measurement (Davies & Anderssen,

139 1997). The interval on which the relaxation spectrum should be determined is $e^{\pi/2}\omega_{\max}^{-1} < \omega^{-1}$
140 $< e^{\pi/2}\omega_{\min}^{-1}$, i.e. shorter than $\omega_{\max}^{-1} < \omega < \omega_{\min}^{-1}$ by 1.36 decades (Davies, et al., 1997).

141 A software platform that is readily available to the experimentalist for numerical
142 calculations of relaxation spectra is MATLAB. There are several MATLAB algorithms that
143 employ the Tikhonov regularization to estimate parameters with the L-curve criterion leading
144 to relaxation spectra derivation (Hansen, 2002; Kontogiorgos, 2010; Kontogiorgos, Jiang, &
145 Kasapis, 2009; Wendlandt, 2005). In the following section, we utilize the most recent version
146 of the program ReSpect v 2.0, which is available with a standalone graphic user interface in
147 MATLAB (Takeh & Shanbhag, 2013) to revisit the relaxation spectra of high-solid
148 hydrocolloid samples from dynamic data in shear.

149

150 **3. Structural relaxation spectra of high-solid hydrocolloid systems**

151 A common approach to increase the experimental timeframe of observation is by
152 constructing the master curve of viscoelasticity at a reference temperature within the glass
153 transition region. This process results in a plot that depicts the effect of molecular motions on
154 the viscoelastic functions for several decades, i.e. beyond the operational frequency range
155 achieved with current instrumentation (typically $0.628 < \omega < 628$ rad/sec). In the present work,
156 we have re-analysed the relaxation spectra of selected high-solid polysaccharides, proteins
157 and their mixed systems in an effort to identify relaxation phenomena.

158 All systems have been prepared using high levels of co-solute (glucose syrup, sucrose or
159 mixtures thereof) and industrially relevant amounts of κ -carrageenan, gellan (Kasapis &
160 Sworn, 2000), pectin at pH 3.0 or 7.0 (Alba, Kasapis, & Kontogiorgos, 2015), gelatin or
161 gelatin/carrageenan mixtures (Kasapis & Al-Marhoobi, 2005), and whey protein (unpublished

162 data). Calculations were performed using the Tikhonov regularization to extract the
163 continuous relaxation spectrum from ω , $G'(\omega)$ and $G''(\omega)$ datasets. The strict criterion for the
164 range of relaxation times was imposed (i.e., $e^{\pi/2}\omega^{-1}_{\max} < \omega^{-1} < e^{-\pi/2}\omega^{-1}_{\min}$) and regularisation
165 parameters were calculated with the L-curve method.

166 Figure 1 shows the outcome of the aforementioned calculations for several high-solid
167 samples. Besides the small-molecule co-solute system of 85% glucose syrup, all hydrocolloid
168 based matrices extend the relaxation to several decades of the predicted timeframe. A
169 qualitative similarity emerges in structural patterns for the high-solid macromolecular
170 networks, and below a characteristic relaxation time of about 0.01 s predicted mechanical
171 spectra seem to converge regardless of physicochemical fingerprint. This characteristic time,
172 usually indicated as τ_o , marks the passage to a short time behavior at the onset of the glassy
173 state and reflects the local segmental motions of the macromolecule following completion of
174 the extended Rouse motions at the end of the glass transition region. In practice, the glassy
175 relaxation of hydrocolloids is negligible and independent of fine structure. This behaviour is
176 also observed in linear and flexible synthetic polymers in the short time regime (Baumgaertel,
177 Schausberger, & Winter, 1990).

178 Above τ_o , samples enter a power law relaxation regime (Figure 1, inset) revealing a non-
179 exponential behaviour whose segmental motions should depend on structural fingerprints and
180 molecular interactions in the condensed matrix (Baumgaertel, et al., 1990; Winter &
181 Chambon, 1986; Winter & Mours, 1997). Power law relaxation has also been observed in
182 low-solid (40%, w/w) gluten composites (Kontogiorgos, Shah, & Bills, 2016; Ng &
183 McKinley, 2008) that follows kinetics characteristic of that non-hydrocolloid system.
184 Discrepancies in spectral decay are observed well into the long-time window of observation in

185 Figure 1. It appears that samples containing monodisperse protein chains relax slower than
186 their polydisperse counterparts of polysaccharides. In the ensuing section, a theoretical
187 framework will be discussed as an avenue of addressing the relationship between structure
188 and physicochemical environment in the relaxation spectrum of hydrocolloid networks.

189

190 **4. Theoretical considerations of structural relaxation in relation to molecular** 191 **interactions**

192 As mentioned earlier, stress relaxation spectra can be used to establish the roadmap of the
193 mechanical glassy state and glass transition region by varying the experimental timescale or
194 frequency of observation. The properties of vitrified materials are associated with changes in
195 free energy, volume, or enthalpy relaxations and a common reference can be made to these
196 quantities in an effort to obtain results with physical meaning (Ferry, 1980). In early
197 investigations of amorphous synthetic polymers and, more recently, in high-solid
198 hydrocolloids, the approach used extensively to develop a fundamental understanding of the
199 mechanical glass transition region is based mainly on the concept of free volume.

200 Free volume is a useful semi quantitative, although somewhat poorly defined, concept
201 closely related to the hole theory of liquids. The total volume per mole, u , is pictured as the
202 sum of the free volume, u_f , and an occupied volume, u_o . Ferry takes u_o as including not only
203 the van der Waals radii but also the volume associated with local vibrational motion of atoms
204 (Ferry, 1991). The free volume is therefore that extra volume required for larger scale
205 vibrational motions than those found between consecutive atoms of the same chain. Flexing
206 over several atoms, that is, transverse string-like vibrations of a chain rather than longitudinal
207 or rotational vibrations will obviously require extra room. The free volume concept is popular

208 partly due to it being intuitively appealing. Often but not invariably, it is able to explain
209 observed trends correctly in synthetic polymers, low molecular weight organic liquids,
210 inorganic compounds, high solid hydrocolloid/co-solute preparations, and is easy for workers
211 in materials science coming from many different backgrounds.

212 The free volume framework that has been incorporated within the Williams, Landel and
213 Ferry (WLF) equation can be used to describe structural relaxation processes for the glass
214 transition region according to the following form (Levine, 2002):

$$215 \quad \log a_T = \log [G(t)(T) / G(t)(T_o)] = - \frac{(B/2.303f_o)(T - T_o)}{(f_o/\alpha_f) + T - T_o} \quad (2)$$

216 At any reference temperature, T_o , equation (2) can include two constants, which relate to the
217 free volume theory as follows:

$$218 \quad C_1^0 = B / 2.303f_o \quad \text{and} \quad C_2^0 = f_o / \alpha_f \quad (3)$$

219 where, the fractional free volume, f_o , is the ratio of free to total volume of the molecule, α_f is
220 the thermal expansion coefficient, and B is usually set to one. Application of the WLF
221 equation to stress relaxation spectra in the glass transition region amounts to more than curve
222 fitting since it is able to predict the mechanical glass transition temperature. This is a turning
223 point where large configurational vibrations requiring free volume in the glass transition
224 region cease to be of overriding importance. At lower temperatures, i.e., below T_g , the need to
225 overcome an energetic barrier for the occurrence of local rearrangements from one state to the
226 other becomes of primary importance, which is known as the glassy state. Progress of
227 viscoelasticity within the glassy state is then described by the predictions of the reaction rate
228 theory as seen in the modified Arrhenius equation (Kasapis, 2008).

229 Recently, there has been a certain opposition in the use of free volume, since, in physics
230 of the densely packed systems intermolecular interactions determine volume but not *vice*
231 *versa*. Thus interactions appear to be more fundamental and the ultimate determining factor of
232 molecular dynamics in these materials. A new concept, “the molecular coupling model”, has
233 been put forward to overcome the oversimplification associated with the application of free
234 volume to the entirety of the glass transition region (Ngai, 2000). In spite of the postulates of
235 the free volume theory that vitrification phenomena are not associated with specific details of
236 chemical structure, it is likely, that in order to follow the development of properties within the
237 (broad) transition region, the theory has been unable to pinpoint the intermolecular
238 cooperative dynamics responsible for the diffusional mobility around the glass transition
239 temperature.

240 To move from a qualitative debate of the appropriateness of theoretical treatment, the
241 stress relaxation modulus, $G(t)$, at constant deformation is used in order to expedite estimation
242 of the relaxation time within the temperature domain of vitrification. Experimental data
243 obtained at different temperatures are superposed by shifting horizontally along the
244 logarithmic time axis to implement the so-called method of reduced variables or time-
245 temperature superposition principle (TTS). Superposition is centred on ~~round~~ (centred "on" or
246 "around" but NOT "round", please keep my edit and don't revert it again to "centred round"
247 which an incorrect phrasal verb) the arbitrary choice of a reference temperature, T_o , a choice
248 that is inconsequential as long as it is confined within the glass transition region (Paramita,
249 Bannikova, & Kasapis, 2015). The empirical superposition of data yields a composite (or
250 master) curve, and good matching of the shapes of adjacent curves must be achieved, a
251 criterion that is critical for the applicability of the method of reduced variables.

252 Superposed values of the stress relaxation modulus, $G_p(t)$, do not change much with time
253 in the rubbery and glassy states, but they do rapidly in the glass transition region, i.e., up to
254 four or five orders of magnitude. Shifting of data generates a set of shift factors, a_T , which are
255 the numerical parameters describing the extent of data reduction, as follows (Mansfield,
256 1993):

$$257 \quad G_p(t) = G(t) T_o \rho_o / T \rho \quad \text{vs.} \quad t/a_T \quad (4)$$

258 where, ρ_o is the density of the material at T_o . In practice, satisfactory matching of adjacent
259 curves is achieved without the vertical shift of the temperature and density factors, since
260 logarithmic density changes of hydrocolloid matrices are relatively small with experimental
261 temperature compared to the rapid changes in viscoelastic functions.

262 An example of stress-relaxation data superposition is reproduced in Figure 2 for part of
263 the composite curve of a gelatin/co-solute sample, which constitutes the extreme short-time
264 segment of the rubber to glass transition (Kasapis, 2006). The approach overcomes the
265 drawbacks of analyzing, with a single model, the entirety of the rubber-to-glass dispersion,
266 which encompasses broad temperature or time domains that activate molecular motions
267 emanating from residual amino acids (monomers) to polymeric segments of considerable
268 length. The gelatin/co-solute system appears to be thermorheologically simple (TS) implying
269 that the major relaxation processes producing the master curve in Figure 2 have the same
270 temperature dependence. This is not a universal observation and, indeed, thermorheological
271 complexity (TC) has been reported on the superposition of stress relaxation spectra in a
272 number of amorphous materials and epoxy resins (Ngai & Plazek, 1995). It has been reported,
273 however, that TC is more pronounced on low molecular weight materials, with the high

274 molecular weight counterparts, as the present gelatin fraction ($M_n = 67,200$), exhibiting good
275 superposition of mechanical data hence leading to thermorheological simplicity.

276 The analysis becomes more explicit considering that even in thermorheologically simple
277 systems the “softening dispersion” of the transition zone unveils a variety of mechanisms
278 from the Gaussian submolecular motions of the extended Rouse model to the local segmental
279 motions. At best, the former accounts for the long time portion of the glass transition region.
280 Interesting physical phenomena, however, leading to the completion of vitrification with
281 decreasing temperature, for example, are related to local segmental motions within the
282 Gaussian submolecule (Huang, Szleifer, & Peppas, 2002). Tobolsky and co-workers first dealt
283 with the motions, which were found to deviate from the predictions of the extended Rouse
284 model, in the vitrification of synthetic polymers (Tobolsky & Aklonis, 1964). Subsequently,
285 it became apparent that the relaxation pattern of these sub-Rouse and local segmental modes
286 at high frequencies or short times of the glass transition region depended on the chemical
287 structure of the macromolecule. For example, the contrasting behaviour of the master curves
288 of polystyrene and polyisobutylene constitute focal points of discussion in this respect.

289 The nature of the local segmental motions is responsible for the glass transition
290 temperature of an individual system, as monitored using several well-established techniques.
291 In particular, the extent of interactions between neighbouring segments relates to the
292 distribution of relaxation times, and can be followed by the so-called stretched exponential
293 function of Kohlrausch, Williams and Watts (KWW) in the time domain (Ngai & Roland,
294 2002):

$$295 \quad \phi(t) = \exp[-(t / \tau)^\beta] \quad (5)$$

296

297 where, τ is the relaxation time. The stretch exponent β can take values between 0 and 1.0 thus
298 imparting a non-exponential character to the kinetics of structural relaxation of synthetic
299 glasses. At the times appropriate for mechanical measurements, equation (5) recasts for the
300 stress relaxation modulus of the present investigation as follows (Ngai, Magill, & Plazek,
301 2000):

$$302 \quad G(t) = (G_g - G_e) \exp[-(t/\tau)^{1-n}] + G_e \quad (6)$$

303 where, G_g is the unrelaxed glassy modulus, G_e is the relaxed or equilibrium modulus of the
304 local segmental motions and t is the time after the application of a fixed strain. The coupling
305 constant, n ($\beta = 1 - n$), ranges from 0 to 1.0 and reflects the intensity of interactions (coupling)
306 between the primitive (underlying) relaxation and the physicochemical environment of the
307 surrounding materials.

308 The KWW function of equation (6) was utilised to fit the stress relaxation data of the
309 gelatin/co-solute sample in Figure 2 at the glass transition temperature ($T_g = -30^\circ\text{C}$) where,
310 besides the local segmental motions, other molecular mechanisms should have a minimal
311 contribution to the relaxation spectrum. Equation (6) is applicable to relaxation patterns
312 reflecting segmental mobility and, therefore, values of experimental functions should fall
313 within the range: $G_g > G(t) > G_e$. Secondary (β) relaxations would be responsible for the
314 region $G(t) > G_g$, whereas extended Rouse-like modes are expected to dominate at $G(t) < G_e$.
315 Values of G_g and G_e were taken to be about 1.5×10^{10} and 3.5×10^9 Pa, respectively. This is in
316 accordance with experience from the synthetic polymer research, e.g., results on unplasticized
317 and plasticized poly(vinyl chloride), where the unrelaxed to relaxed modulus ratio is between
318 4.0 and 4.5, and modeling provides an adequate fit of the short-time section of the normalized
319 spectrum (Ngai, 1999).

320 As shown in Figure 3, the two-parameter KWW function follows well the progression of
321 superposed stress relaxation data reflecting the local segmental motion and returns τ and n
322 values of $\approx 0.2 \times 10^{-4}$ s and 0.57 for the gelatin/co-solute preparation at -30 °C. The higher
323 the value of n , the stronger the intermolecular coupling, which originates from the chemical
324 structure of the macromolecule and its surrounding environment. Experimentally, it was
325 found that the n values of strongly interlinking or sterically interfering chains of synthetic
326 materials range between 0.66 and 0.77 (e.g., poly(vinyl chloride), poly(methylmethacrylate))
327 (Hutchinson, 1995). Work on the biological glass of gelatin/co-solute estimates a coupling
328 constant of 0.57 (Kasapis, 2006). This is reasonable, in view of the non-aggregating nature of
329 the gelatin molecule, and the recent finding in the literature that a decrease in the surface of
330 contact between the protein and polyhydroxyl co-solute is necessary to induce
331 thermodynamically favourable conditions in the mixture.

332 Treating a single molecular-weight fraction of gelatin with the combined framework of
333 coupling theory/non-exponential KWW equation encouraged further explorations in the
334 structural properties of biological glasses. A logical sequel of the aforementioned approach
335 was to examine its applicability to the first four extracts of the protein from a single batch of
336 cowhide produced by alkaline hydrolysis of collagen (type B). These are noted here as PC1,
337 PC2, PC3 and PC4, with the weight average molecular weights (M_w) of the four fractions
338 from PC1 to PC4 being 317.7, 283.6, 228.9 and 197.4 kD, respectively. Fitting the master
339 curves of superposed stress relaxation modulus with the KWW equation allows estimation of
340 coupling constants, which range from 0.549 to 0.582 (Jiang, Kasapis, & Kontogiorgos, 2012).
341 This treatment of mechanical data *via* KWW modeling is shown in Figure 3, which produces
342 increasingly higher values of the coupling constant with gelatin molecular weight.

343 That was the first demonstration of a specific relationship between coupling constant and
344 molecular weight of a high-solid hydrocolloid preparation. The higher the value of coupling
345 constant the stronger the intermolecular coupling, an outcome which invites comparison with
346 data from other systems found in the literature. This is facilitated by considering the structural
347 properties of the glass dispersion in high-solid gelling polysaccharides. Work was carried out
348 in systems of 2.0% agarose plus 78.0% glucose syrup, 0.5% κ -carrageenan plus 79.5%
349 glucose syrup at 10 mM added KCl, and 1.0% deacylated gellan plus 79.0% glucose syrup at
350 7.5 mM added CaCl_2 . KWW modeling of stress relaxation data for the three polysaccharide
351 samples at their short-time end of the glass transition region yielded n values between 0.59
352 and 0.64 (Jiang, et al., 2011). Therefore, the estimates for gelatin, in terms of the increasing
353 values of the coupling constant with molecular weight that facilitates structure formation, are
354 reasonable compared to the corresponding n values for vitrified polysaccharide matrices.

355 Polysaccharides have highly persistent backbone geometry, in comparison to the flexible
356 and non-aggregating gelatin chain, which should enhance interactions between adjacent
357 macromolecules (Kasapis, 2005). In addition, polysaccharides exhibit distinct topology from
358 that of gelatin, which micro phase separates in mixture with polyhydroxyl compounds, with
359 their networks effectively being dissolved within the saturated co-solute environment
360 (Kasapis, Al-Marhoobi, Deszczynski, Mitchell, & Abeysekera, 2003). Such distinct topology
361 should further enhance interactions between macromolecules and surrounding
362 physicochemical environment in polysaccharide/co-solute mixtures seen in higher values of
363 the coupling constant, as compared to the estimates for the gelatin/co-solute system.

364

365

366 **5. Conclusions**

367 We have reviewed structural relaxation spectra from the literature in an effort to evaluate
368 the application of current theoretical frameworks to mechanical variation recorded through the
369 rubber to glass transition region. Discussion focused mainly on gelling polysaccharide/co-
370 solute systems, four distinct molecular fractions of gelatin in mixture with co-solute and whey
371 protein samples in comparison with corresponding work from amorphous synthetic polymers.
372 This type of analysis is obviated by the broad range of experimental times of stress relaxation
373 recorded in isothermal tests over temperatures that traverse the softening dispersion.
374 Utilization of the method of reduced variables proved successful in superposing experimental
375 data to yield master curves of mechanical profiles that separate the basic functions of time and
376 temperature in hydrocolloid relaxation.

377 Fundamental insights into the local segmental motions responsible for intermolecular
378 interactions in the vicinity of the glass transition temperature were gained by calculation of
379 the stress relaxation spectra. Interactions with the surrounding physicochemical environment
380 yield relaxation times below 0.01 sec, an outcome that reflects the rapid local segmental
381 motions of hydrocolloid chains. The molecular coupling theory of cooperativity was used to
382 predict the extent of coupling in adjacent interactions, which was found to increase with
383 molecular weight of high-solid gelatin fractions. Comparisons were afforded with the
384 coupling constants of other macromolecules (gelling polysaccharides and amorphous
385 synthetics) based on backbone conformational mobility or pendant-group rotational mobility.
386 It remains to be seen if comparable levels of understanding achieved for the gelatin/co-solute
387 mixture can be reached in relation to the molecular weight of polysaccharides, which exhibit

388 distinct three-dimensional morphology from that of the protein in condensed mixtures with
389 co-solute.

390

391

392

393

394

395

396

397

398

399

400

401

402

403

404

405

406

407

408

409

410

411 **References**

- 412 Alba, K., Kasapis, S., & Kontogiorgos, V. (2015). Influence of pH on mechanical relaxations
413 in high solids LM-pectin preparations. *Carbohydrate Polymers*, *127*, 182-188.
- 414 Bae, J.-E., & Cho, K. S. (2015). Logarithmic method for continuous relaxation spectrum and
415 comparison with previous methods. *Journal of Rheology*, *59*, 1081-1112.
- 416 Baumgaertel, M., Schausberger, A., & Winter, H. H. (1990). The relaxation of polymers with
417 linear flexible chains of uniform length. *Rheologica Acta*, *29*, 400-408.
- 418 Baumgaertel, M., & Winter, H. H. (1989). Determination of discrete relaxation and
419 retardation time spectra from dynamic mechanical data. *Rheologica Acta*, *28*, 511-519.
- 420 Ciocci Brazzano, L., Pellizza, L. J., Matteo, C. L., & Sorichetti, P. A. (2016). A Bayesian
421 method for analysing relaxation spectra. *Computer Physics Communications*, *198*, 22-
422 30.
- 423 Davies, A. R., & Anderssen, R. S. (1997). Sampling localization in determining the relaxation
424 spectrum. *Journal of Non-Newtonian Fluid Mechanics*, *73*, 163-179.
- 425 Elster, C., & Honerkamp, J. (1991). Modified maximum entropy method and its application to
426 creep data. *Macromolecules*, *24*, 310-314.
- 427 Elster, C., Honerkamp, J., & Weese, J. (1991). Using regularization methods for the
428 determination of relaxation and retardation spectra of polymeric liquids. *Rheologica
429 Acta*, *30*, 161-174.
- 430 Ferry, J. D. (1980). *Viscoelastic properties of polymers* (3rd ed.). New York: Wiley.
- 431 Ferry, J. D. (1991). Some reflections on the early development of polymer dynamics:
432 viscoelasticity, dielectric dispersion, and self-diffusion. *Macromolecules*, *24*, 5237-
433 5245.
- 434 Hansen, P.-C. (1992). Analysis of discrete ill-posed problems by means of the L-curve. *SIAM
435 Review*, *34*, 561-580.
- 436 Hansen, P.-C. (2002). Regtools. In
- 437 Huang, Y., Szleifer, I., & Peppas, N. A. (2002). A Molecular Theory of Polymer Gels.
438 *Macromolecules*, *35*, 1373-1380.
- 439 Hutchinson, J. M. (1995). Physical aging of polymers. *Progress in Polymer Science*, *20*, 703-
440 760.
- 441 Jensen, E. A. (2002). Determination of discrete relaxation spectra using Simmulated
442 Annealing. *Journal of Non-Newtonian Fluid Mechanics*, *107*.
- 443 Jiang, B., Kasapis, S. & Kontogiorgos, V. (2012). Fundamental considerations in the effect of
444 molecular weight on the glass transition of the gelatin/co-solute system. *Biopolymers*,
445 *97*, 303-310.
- 446 Kasapis, S. (2005). Composition and Structure-Function Relationships in Gums. In Y. H. Hui
447 (Ed.), *Handbook of Food Science, Technology, and Engineering - 4 Volume Set*: CRC
448 Press.
- 449 Kasapis, S. (2006). Building on the WLF/Free Volume Framework: Utilization of the
450 Coupling Model in the Relaxation Dynamics of the Gelatin/Cosolute System.
451 *Biomacromolecules*, *7*, 1671-1678.
- 452 Kasapis, S. (2008). Recent Advances and Future Challenges in the Explanation and
453 Exploitation of the Network Glass Transition of High Sugar/Biopolymer Mixtures.
454 *Critical Reviews in Food Science and Nutrition*, *48*, 185-203.

455 Kasapis, S., & Al-Marhoobi, I. M. (2005). Bridging the Divide between the High- and Low-
456 Solid Analyses in the Gelatin/κ-Carrageenan Mixture. *Biomacromolecules*, 6, 14-
457 23.

458 Kasapis, S., Al-Marhoobi, I. M., Deszczynski, M., Mitchell, J. R., & Abeysekera, R. (2003).
459 Gelatin vs Polysaccharide in Mixture with Sugar. *Biomacromolecules*, 4, 1142-1149.

460 Kasapis, S., & Sworn, G. (2000). Separation of the variables of time and temperature in the
461 mechanical properties of high sugar/polysaccharide mixtures. *Biopolymers*, 53, 40-45.

462 Kontogiorgos, V. (2010). Calculation of relaxation spectra from mechanical spectra in
463 MATLAB. *Polymer Testing*, 29, 1021-1025.

464 Kontogiorgos, V., Jiang, B., & Kasapis, S. (2009). Numerical computation of relaxation
465 spectra from mechanical measurements in biopolymers. *Food Research International*,
466 42, 130-136.

467 Kontogiorgos, V., Shah, P., & Bills, P. (2016). Influence of supramolecular forces on the
468 linear viscoelasticity of gluten. *Rheologica Acta*, 1-9.

469 Levine, H. (2002). Appendix I: Summary report of the discussion symposium on chemistry
470 and application technology of amorphous carbohydrates. In H. Levine (Ed.),
471 *Amorphous Food and Pharmaceutical Systems* (pp. P010-P026): The Royal Society of
472 Chemistry.

473 Mansfield, M. L. (1993). An overview of theories of the glass transition. In J. M. V.
474 Blanshard & P. Lillford (Eds.), *The Glassy State in Foods* (pp. 103-122): Nottingham
475 University Press.

476 McDougall, I., Orbey, N., & Dealy, J. M. (2014). Inferring meaningful relaxation spectra
477 from experimental data. *Journal of Rheology*, 58, 779-797.

478 Ng, T. S. K., & McKinley, G. H. (2008). Power law gels at finite strains: The nonlinear
479 rheology of gluten gels. *Journal of Rheology*, 52, 417-449.

480 Ngai, K. L. (1999). Synergy of entropy and intermolecular coupling in supercooling liquids.
481 *The Journal of Chemical Physics*, 111, 3639-3643.

482 Ngai, K. L. (2000). Dynamic and thermodynamic properties of glass-forming substances.
483 *Journal of Non-Crystalline Solids*, 275, 7-51.

484 Ngai, K. L., Magill, J. H., & Plazek, D. J. (2000). Flow, diffusion and crystallization of
485 supercooled liquids: Revisited. *The Journal of Chemical Physics*, 112, 1887-1892.

486 Ngai, K. L., & Plazek, D. J. (1995). Identification of Different Modes of Molecular Motion in
487 Polymers That Cause Thermorheological Complexity. *Rubber Chemistry and*
488 *Technology*, 68, 376-434.

489 Ngai, K. L., & Roland, C. M. (2002). Development of cooperativity in the local segmental
490 dynamics of poly(vinylacetate): synergy of thermodynamics and intermolecular
491 coupling. *Polymer*, 43, 567-573.

492 Paramita, V. D., Bannikova, A., & Kasapis, S. (2015). Release mechanism of omega-3 fatty
493 acid in κ-carrageenan/polydextrose undergoing glass transition. *Carbohydrate*
494 *Polymers*, 126, 141-149.

495 Provencher, S. W. (1982). Contin - a General-Purpose Constrained Regularization Program
496 for Inverting Noisy Linear Algebraic and Integral-Equations. *Computer Physics*
497 *Communications*, 27, 229-242.

498 Rezghi, M., & Hosseini, S. M. (2009). A new variant of L-curve for Tikhonov regularization.
499 *Journal of Computational and Applied Mathematics*, 231, 914-924.

500 Rubinstein, M., & Semenov, A. N. (2001). Dynamics of Entangled Solutions of Associating
501 Polymers. *Macromolecules*, *34*, 1058-1068.

502 Soo Cho, K., & Woo Park, G. (2013). Fixed-point iteration for relaxation spectrum from
503 dynamic mechanical data. *Journal of Rheology*, *57*, 647-678.

504 Stadler, F. J., & Bailly, C. (2009). A new method for the calculation of continuous relaxation
505 spectra from dynamic-mechanical data. *Rheologica Acta*, *48*, 33-49.

506 Takeh, A., & Shanbhag, S. (2013). A computer program to extract the continuous and discrete
507 relaxation spectra from dynamic viscoelastic measurements. *Applied Rheology*, *23*.

508 Tikhonov, A. N., Goncharsky, A., Stepanov, V. V., & Yagola, A. G. (1995). *Numerical*
509 *Methods for the Solution of Ill-Posed Problems*. London: Springer.

510 Tobolsky, A. V., & Aklonis J. J. (1964). A molecular theory for viscoelastic behavior of
511 amorphous polymers. *J. Phys. Chem.*, *68* , 1970–1973

512 Wendlandt, M. (2005). NLCSmoothReg. In.

513 Winter, H. H. (1997). Analysis of dynamic mechanical data: inversion into a relaxation time
514 spectrum and consistency check. *Journal of Non-Newtonian Fluid Mechanics*, *68*,
515 225-239.

516 Winter, H. H., & Chambon, F. (1986). Analysis of Linear Viscoelasticity of a Crosslinking
517 Polymer at the Gel Point. *Journal of Rheology*, *30*, 367-382.

518 Winter, H. H., & Mours, M. (1997). Rheology of Polymers Near Liquid-Solid Transitions. In
519 *Neutron Spin Echo Spectroscopy Viscoelasticity Rheology* (Vol. 134, pp. 165-234):
520 Springer Berlin Heidelberg.

521

522

523

524

525

526

527

528

529

530

531

532

533

534

535

536 **FIGURE LEGENDS**

537

538 **Figure 1:** Relaxation spectra of high-solid hydrocolloid systems, which are divided into two
539 regions: a short-time glassy regime where relaxation is insignificant and a power law glass-
540 transition region that depends on hydrocolloid structure, with the inset depicting an idealized
541 schematic with the relaxation time of local segmental motions.

542

543 **Figure 2:** Short-time part of the stress-relaxation master curve for 15% gelatin, 31.5%
544 glucose syrup and 31.5% sucrose at the reference temperature of -30°C , with the solid line
545 following the predictions of the stretched exponential KWW function (with permission from
546 Kasapis, 2006).

547

548 **Figure 3:** Coupling constant variation plotted against weight-average molecular weight for
549 four gelatin fractions (PC1 to PC4) of 15% protein and 65% glucose syrup (with permission
550 from Jiang, Kasapis & Kontogiorgos, 2012).

551

552

553

554

555

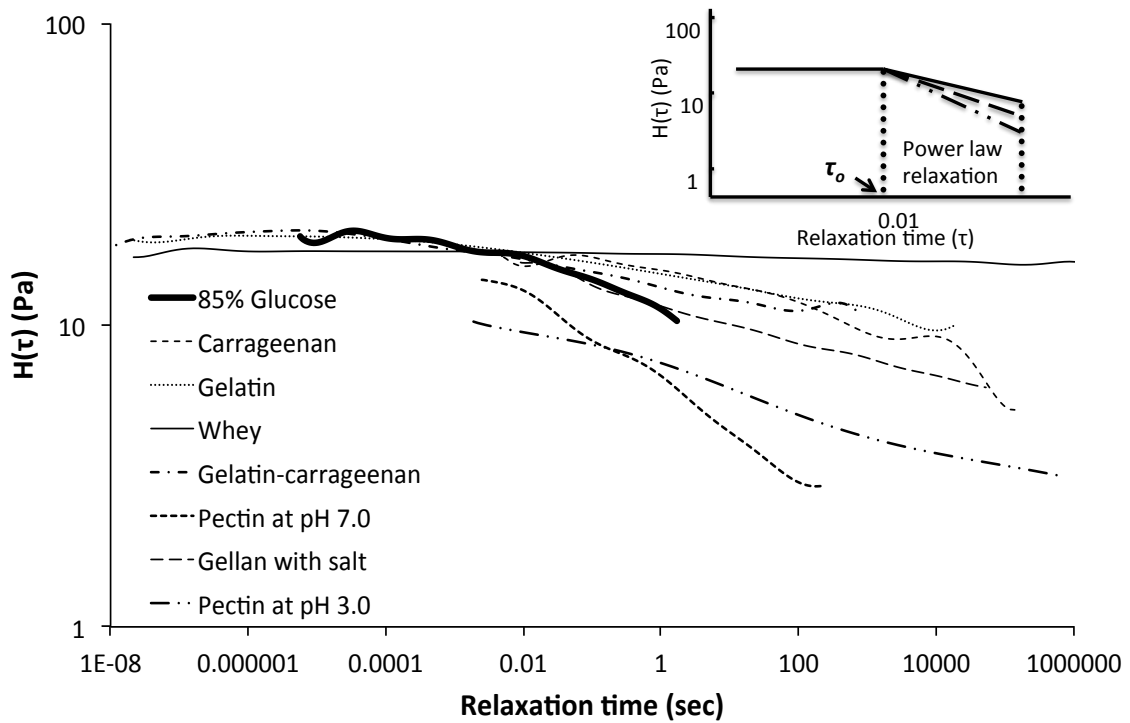
556

557

558

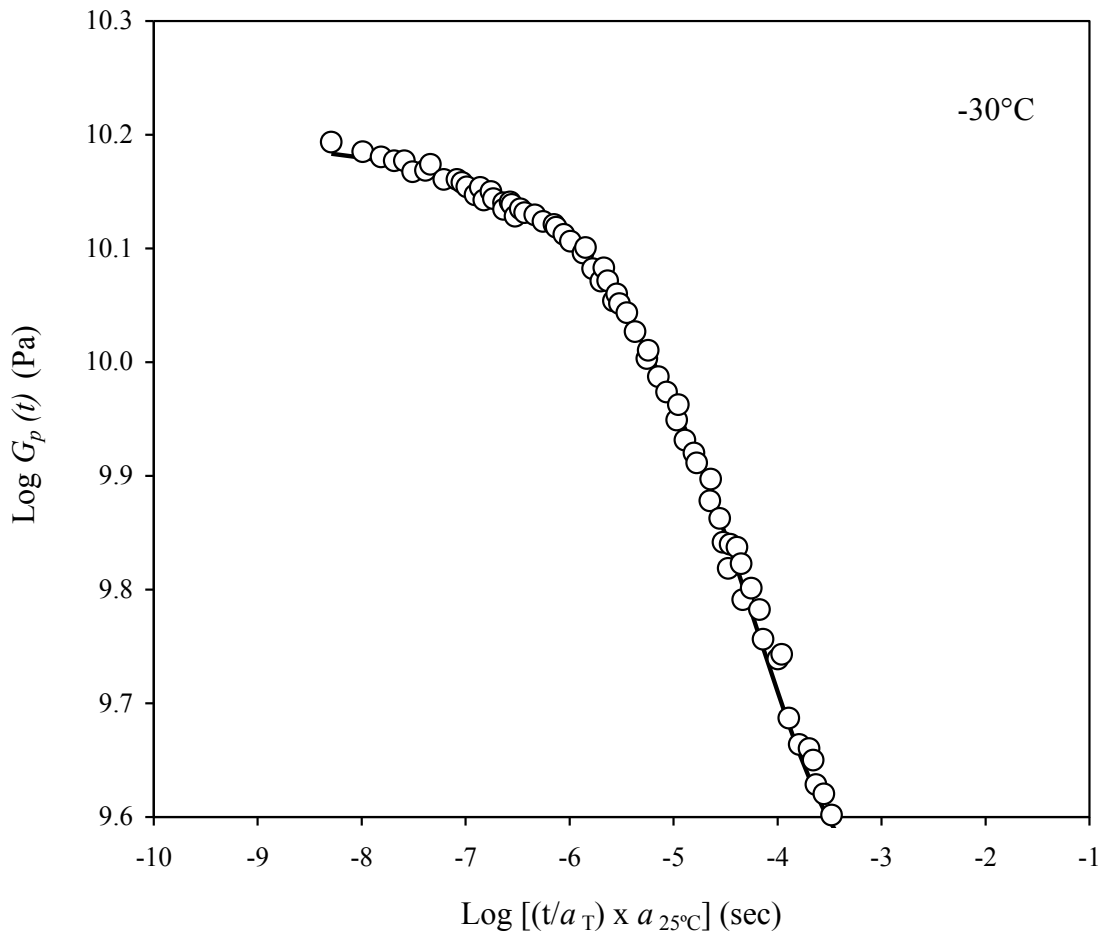
559

560
561
562
563
564
565



566
567
568
569
570
571
572
573
574

Figure 1



575

576

577

578 **Figure 2**

579

580

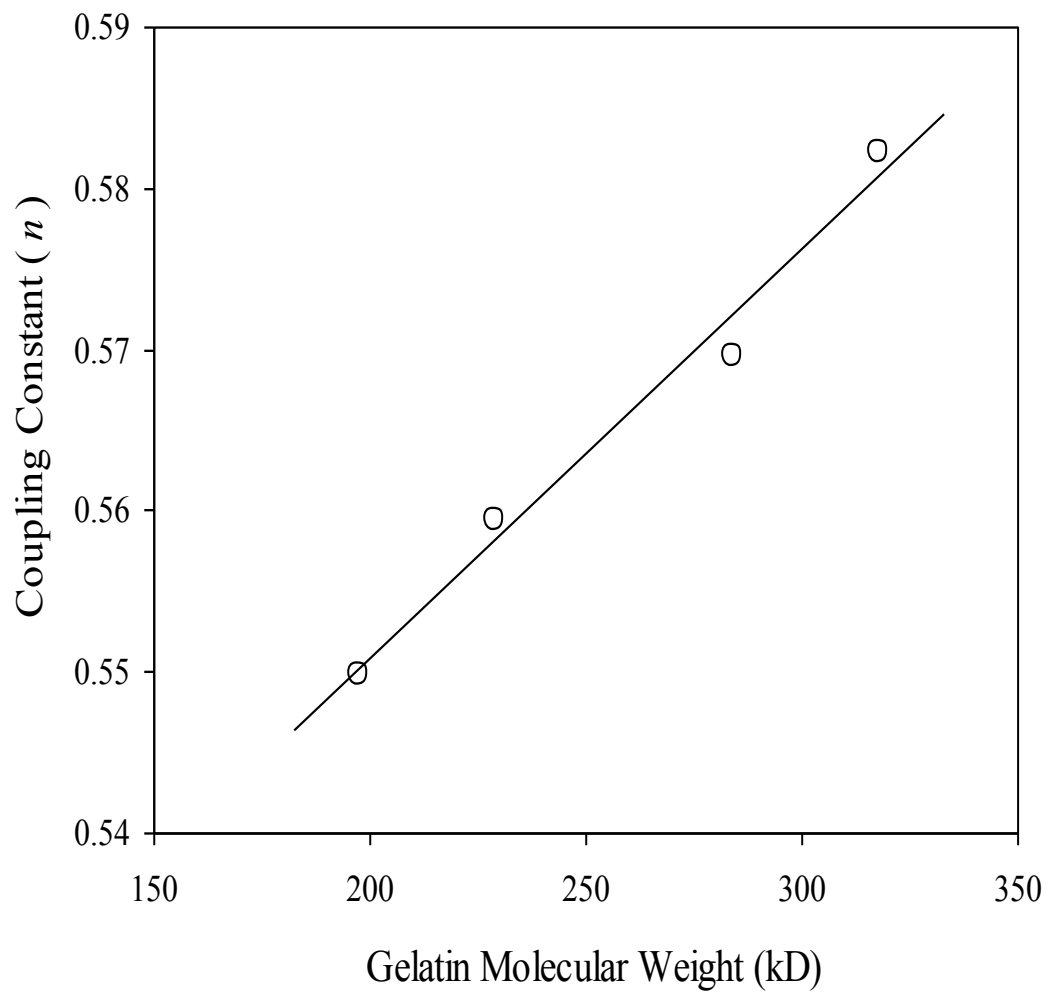
581

582

583

584

585



586

587

588

589 **Figure 3**

590

591

592